SOILS AND FOUNDATIONS Vol. 44, No. 1, 57–69, Feb. 2004
Japanese Geotechnical Society

RATICOSA TUNNEL, ITALY: CHARACTERIZATION OF TECTONIZED CLAY-SHALE AND ANALYSIS OF MONITORING DATA AND FACE STABILITY

DANIELA BOLDINI[i], ALESSANDRO GRAZIANI[ii] and RENATO RIBACCHI[iii]

ABSTRACT

The Raticosa Tunnel (Italy) is one of several tunnels currently under construction for the new Bologna-Florence high-speed railway line. The tunnel, having an overburden of up to 500 m, is located in the Apennine range and half of its 10 km length crosses a tectonized clay-shale formation known as "Chaotic Complex". The construction method is based on full face excavation combined with face reinforcement by means of fiber-glass dowels. Primary lining consists of a shotcrete layer and closed-ring steel sets. Due to heavy squeezing ground conditions, as predicted in the preliminary investigation phase, the excavation of the tunnel was performed under the strict control of an extensive monitoring system.

The paper presents an overview of the physical and mechanical parameters of the Raticosa shale, summarizing the results of laboratory and in situ tests. Face "extrusion" and tunnel wall displacements recorded during the excavation advance have been analyzed and correlated with construction stages. The displacements measured near the tunnel face generally confirm the validity of the design criteria of face reinforcement and early invert closure, which assures tunnel stability before casting the final lining. Large, time-dependent, deformations of ground have generally been recorded, causing local failure phenomena at some locations along the tunnel route. A tentative explanation of the observed behavior has been proposed on the basis of empirical models. Finally, the effect of fiber-glass dowels on face stability has been evaluated by using limit analysis.

Key words: clay-shale, face stability, fiber-glass dowels, monitoring system, tunneling (**IGC**: C9/G5/H5)

THE RATICOSA TUNNEL

The Raticosa tunnel (10 km) is one of the tunnels currently under construction for the new high-speed railway line which crosses the Apennine range between Bologna and Florence (Italy) (Lunardi and Focaracci, 1999; Gambelli, 1999). Starting from the Bologna side, half the tunnel has been excavated in a tectonized clay shale formation known as "Chaotic Complex" which, right from the design stage, has represented one of the most critical points in the development of the whole project due to the poor geotechnical conditions and a high overburden of up to 500 m (Fig. 1). The same formation is also crossed by the Osteria access tunnel, which runs almost parallel to the main tunnel before turning to intersect it.

Due to expected squeezing ground conditions, full face-excavation required face reinforcement by means of fiber-glass dowels. Primary lining consisted of a shotcrete layer and closed-ring steel sets.

Tunnel deformation and loading conditions of the lining were carefully monitored during tunneling so as to ensure compliance with construction quality requirements, verify the design assumptions and calibrate both reinforcement pattern at the face and the strength required for the primary lining. Moreover, the large amount of data gathered during construction represents a valuable tool for back-analysis of the mechanical behavior of the tectonized clay-shale for which geotechnical characterization in the preliminary investigation stage was difficult and affected by many uncertainties.

Geological Framework

Tectonized clay shale formations are rather widespread throughout Southern and Central Italy (e.g., AGI, 1985; Picarelli et al., 2002). The Chaotic Complex encountered during the excavation of the Raticosa tunnel belongs to the Liguridi units and reached the current position after intensive tectonic events which took place from the Miocene-Pliocene to the Plio-Pleistocene.

The chaotic structure of the formation is the result of such tectonic actions. Lithologically the Raticosa shale is mainly composed of a pelitic matrix with dispersed lithic components.

[i] Research Associate, Ph.D., University of Rome "La Sapienza", Department of Structural and Geotechnical Engineering, via Monte d'Oro 28, 00186 Rome, Italy (daniela.boldini@uniroma1.it).
[ii] Research Associate, Ph.D., ditto (alessandro.graziani@uniroma1.it).
[iii] Professor, ditto (renato.ribacchi@uniroma1.it).
Manuscript was received for review on January 20, 2003.
Written discussions on this paper should be submitted before September 1, 2004 to the Japanese Geotechnical Society, Sugayama Bldg. 4F, Kanda Awaji-cho 2-23, Chiyoda-ku, Tokyo 101-0063, Japan. Upon request the closing date may be extended one month.

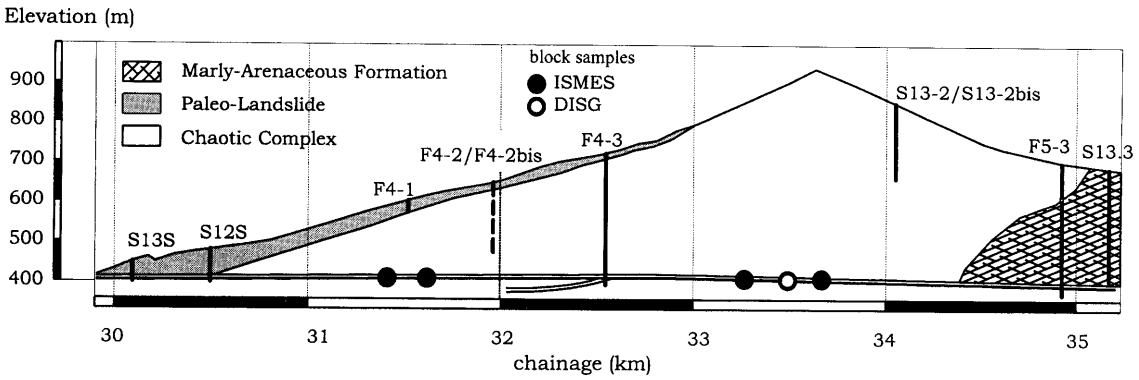

Fig. 1. Geological profile along the tunnel route and location of boreholes and blocks taken during tunnel excavation

Table 1. Results of the X-ray diffraction analysis

Borehole/Block		S12-S		F4-2		DISG	
Depth h (m)		82		150		496	
Quartz + Feldspars (%)		17 ~ 22		41		30 ~ 38	
Carbonates (%)		35 ~ 40		0		30 ~ 35	
Phyllo-silicates (%)	Kaolinite (%)	40 ~ 45	<2	49	2 ~ 12	25 ~ 30	<5
	Chlorite (%)		6 ~ 7		2 ~ 12		<5
	Illite (%)		21 ~ 32		12 ~ 25		15 ~ 20
	Illite-Smectite (%)		2 ~ 11		12 ~ 25		
Others (%)		0		10		4 ~ 8	

The pelitic matrix is constituted by a tight assemblage of hard clay scales of a size of millimeters to centimeters whose surfaces are curved, smooth and at times striated.

Figure 1 shows the location of the boreholes drilled during the investigation phase and of the blocks taken at the tunnel face during the excavation. Samples from the boreholes and blocks denominated as ISMES were taken and tested in the laboratory by the ISMES company on behalf of the contractor CAVET, which also provided the authors with all the available results of the geotechnical investigations carried out at the design stage. The block denominated as DISG was taken during tunnel excavation and used for geotechnical characterization at the geotechnical laboratory of the Department of Structural and Geotechnical Engineering (University of Rome "La Sapienza").

A semi-quantitative mineralogical composition (Table 1) has been obtained by X-ray diffraction (XRD) analysis on several clay-shale samples taken at different depths from boreholes S12S and F4-2 and from the DISG block directly cut from the tunnel face. Mineral composition has been found to vary greatly in the three analyzed samples even if only the total fraction of clay minerals is considered. The deeper sample is characterized by a remarkably lower phyllo-silicate content (25 ~ 30% of the total dry weight), which increases to 45% for the more shallow samples. The most highly swelling clay mineral, i.e. smectite, is present in small proportions in the form of alternating illite-smectite layers.

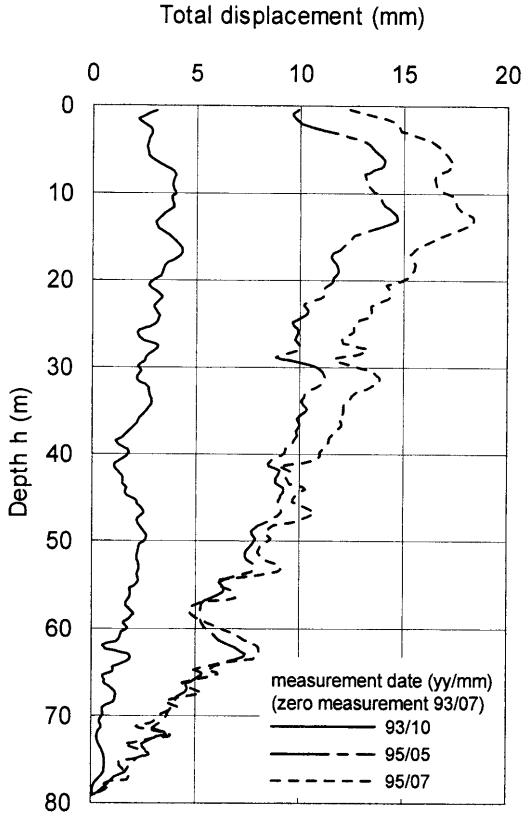

Fig. 2. Total displacements measured in inclinometer borehole S12S

The lithic components include calcareous, marly and arenaceous fragments for a total volume fraction varying between 0 and 20 ~ 30%. Because of the low percentage of the lithic components, mainly present in the form of disarranged strata and fragments, the mechanical behavior of the Chaotic Complex at the macroscale is governed by the clay shale matrix.

The northern stretch of the Raticosa tunnel (Bologna side) crosses a large paleo-landslide area for approximately 500 m (Fig. 1), where deformation phenomena are still active. Movements of more than 4 mm/year were measured in the 1993–95 period (i.e., before tunnel excavation) at the surface of the landslide body along borehole S12S equipped with an inclinometer tube

Table 2. Index and mechanical properties of the Raticosa clay-shale

Properties	Range	Average
Unit weight of total volume γ (kN/m^3)	20.8 ~ 24.1	22.8
Unit weight of solid γ_s (kN/m^3)	26.7 ~ 27.7	27.5
Natural water content w (%)	2 ~ 19	9
Liquid limit w_L (%)	30 ~ 48	38
Plastic limit w_P (%)	16 ~ 22	18
Saturation degree S_r (%)	48 ~ 94	77
Clay fraction CF (%)	3 ~ 44	20
Compression index C_c	0.10 ~ 0.17	0.12
Swelling index C_s	0.03 ~ 0.06	0.05
P-wave velocity V_P (m/s)	2000 ~ 2500	
S-wave velocity V_S (m/s)	1000 ~ 1100	
Triaxial peak cohesion c'_p (kPa)*	16 ~ 540	
Triaxial peak friction angle φ'_p	15°	
Direct shear peak (residual) cohesion (kPa)	170 (80)	
Direct shear peak (residual) friction angle	14° (10°)	

* The lower and upper limits refer to values obtained from samples taken at depths h below or above 200 m.

(Fig. 2). More recent measurements exhibit a more random trend, difficult to be soundly assessed. Moreover, the last measurements have been limited to the first 60 m since the inclinometer probe could not be moved further down.

Geotechnical Characterization

Geotechnical characterization of the clay-shale formation has met many difficulties and uncertainties, mainly related to the high sensitivity to sampling disturbance and specimen preparation of the pervasively fissured hard material. A summary of the basic geotechnical parameters evaluated for the tectonized clay shale is given in Table 2.

The in situ measurement of hydraulic conductivity by borehole pumping tests has failed because of negligible water absorption, indicating, nevertheless, very low bulk permeability, less than 10^{-11} m/s. Only inside the more permeable and loosened material of the paleo-landslide mass could meaningful pumping tests be executed, obtaining permeability values in the range of $3 \times 10^{-7} \sim 2 \times 10^{-9}$ m/s.

At present no reliable information is available on pore pressure distribution inside the Chaotic Complex; still, it is reasonable to assume that the water table is at the ground surface and that the whole formation is almost fully saturated.

Piezometers installed in the ground during tunnel excavation (14 electric instruments up to a distance of 15 m from the tunnel wall) have not measured any pore water pressure so far.

Two Casagrande piezometers installed in borehole

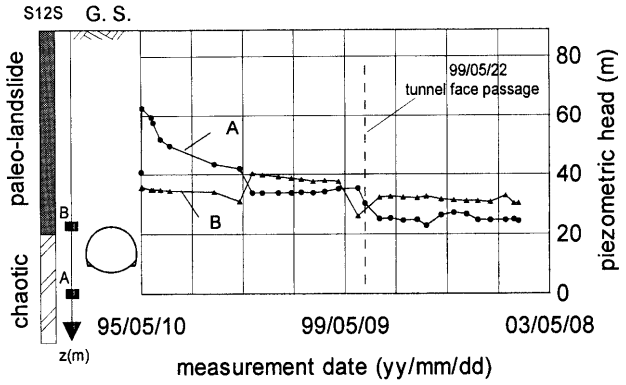

Fig. 3. Hydraulic head measured by two Casagrande piezometers in borehole S12S

S12S inside the paleo-landslide area have recorded a piezometric head which is variable along the vertical and, in any case, lower than the depth of the measuring points from the ground surface (Fig. 3). The deeper piezometer (A) shows a continuously time-decreasing trend of pore pressure with a steeper gradient as the tunnel face approaches the borehole position; piezometer (B), located in the transition zone at the boundary of the paleo-landslide, exhibits a more irregular trend, probably influenced by deformation phenomena that are still active.

The lack of valuable information about pore pressure distribution leads to much uncertainty about the effective stress field at the depth of the tunnel.

The index properties obtained on borehole cores (according to the ASTM D 421-58 procedure) do not vary significantly neither with position along the tunnel route, nor with depth (Fig. 4). The clay-shale blocks taken at the tunnel face give more scattered results, especially the deeper samples. The natural water content w (average value 9%) is always lower than the plastic limit w_P.

Only three values of the index properties are available for the paleo-landslide area; basically, the unit weight of total volume γ seems to be lower than that obtained for the deeper material and the natural water content w tends to reach the plastic limit w_P.

The index properties (particularly w_L and PI) and the grain-size distribution of the hardened clay scales strongly depend on the disaggregating technique adopted in preparing the samples. Only prolonged working with the spatula will destroy most of the diagenetic bonds within the shear lenses, thereby increasing the clay fraction (e.g., Picarelli et al., 2002). Actually, this could be less true for the clay-shales belonging to the Liguridi Units (AGI, 1985), characterized by high carbonate content as is the case of the Raticosa clay-shales (Table 1). An attempt to verify the influence of the disaggregating technique has been made on material taken from the DISG block; the clay fraction has been found to increase from 13% to 23% both after prolonged working with the spatula and after repeated drying and wetting cycles, thus indicating a considerable de-bonding effect similar but still lower than that associated with the transition from the deep clay-

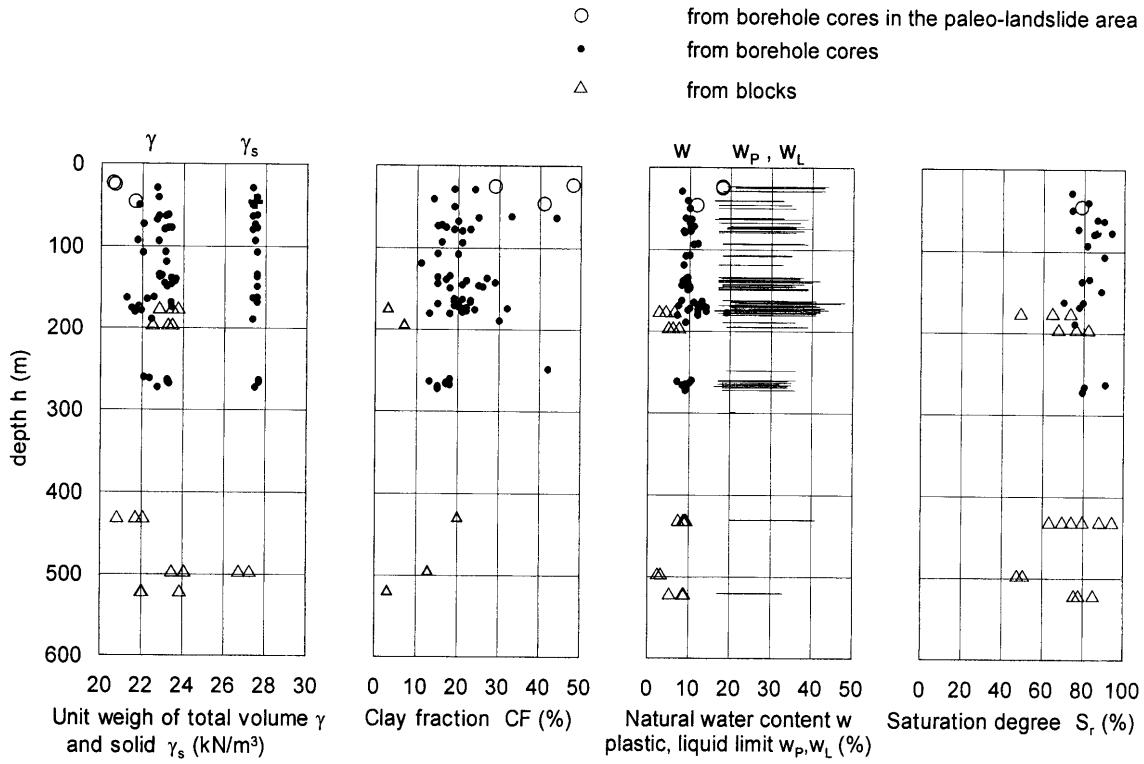

Fig. 4. Index and mechanical properties of the Raticosa clay shale

shale to the completely softened and destructured clay of the landslide mass.

The saturation degree is generally lower than unity also for very deep samples (Fig. 4): this is quite a common finding in scaly clay formations, partly explained by the opening of fissures due to the effect of loosening and stress release during sampling, particularly remarkable for deep samples.

A rough estimate of the sampling disturbance can be obtained by analyzing the result of the Huder-Amberg one-dimensional swelling test (Wittke, 2000). Figure 5 shows the typical result of a test carried out on a sample taken from a deep block ($h = 430$ m); the reduction in the void ratio ($\Delta e \cong 0.1$) between point A (start of the first loading phase) and point C (end of unloading) can be essentially attributed to the closure of fissures previously opened after sampling disturbance, which reduced the saturation degree to about 70%. Due to the negligible volume increase recorded after adding water (point D, before unloading), a swelling pressure $\sigma_0 \leq 7$ MPa can be estimated.

During unloading, with water allowed to penetrate into the sample, swelling deformation is considerable and comparable with that observed in ordinary oedometer tests (Fig. 6). In fact, as often occurs with scaly clays, the Raticosa shale exhibits a very high swelling index C_s and therefore also a high ratio between the swelling index and the compression index (Table 2).

P-wave and S-wave velocities (V_P, V_S) measured on shale blocks taken at the face under an overburden of 480 m showed a dynamic shear modulus of around 2900 MPa; V_P values ranging from 2000 to 2500 m/s were

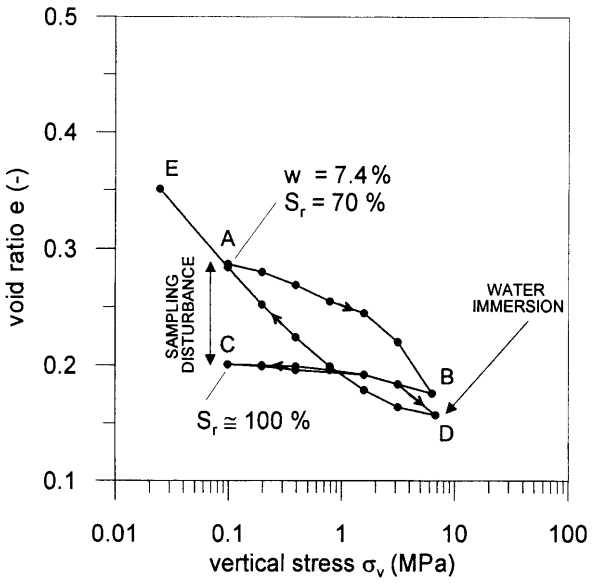

Fig. 5. Results of the Huder-Amberg swelling test (ISMES block from 430 m depth)

measured in boreholes at a depth of around 150 m as well. The dynamic stiffness can be considered an upper limit of the actual in situ stiffness of the rock-mass subjected to excavation-induced loads.

The loading-unloading moduli given by pressuremeter tests appear to be strongly scattered (Fig. 7): the average secant shear modulus $G_{1\text{-}2}$ for the first loading step is about 500 MPa, while the corresponding unloading modulus is about 1.5 times greater.

The reduction in stiffness as unloading proceeds, which

closely resembles the typical mechanical behavior of loosened jointed rock masses, can be mainly related to the mobilization of shear displacements along discontinuities. It is therefore difficult to identify a true elastic modulus. The best estimate should be given by the upper range of the unloading shear moduli.

The presence of the network of fissures strongly affects also the shear strength of the tectonized shale. To evaluate the strength parameters of the shales of the Raticosa tunnel, triaxial as well as direct shear tests were performed on specimens obtained from samples from investigation boreholes as well as from blocks directly taken at the tunnel face (Fig. 8).

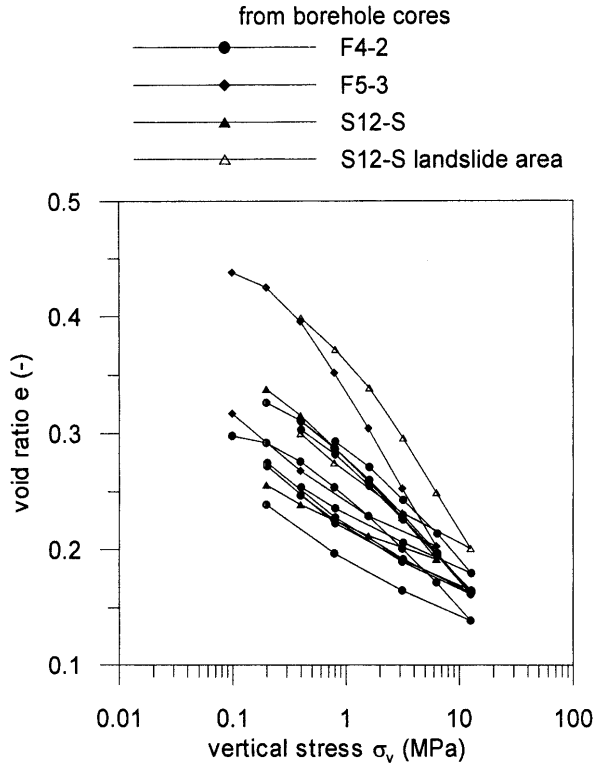

Fig. 6. Results of oedometer compression tests (samples from boreholes F4-2, F5-3, and S12-S)

Triaxial tests (CID and CIU tests) are deemed to afford the more reliable results: in fact data interpolation by a linear Mohr-Coulomb criterion is characterized by a correlation coefficient as high as 0.97. More precisely, peak shear strength data seem to indicate two different strength envelopes according to the depth of the sample, with a much higher cohesion for the samples taken at depths where $h > 200$ m. Beyond peak strength only weak strain-softening is generally observed; a more brittle response has sometimes been observed for specimens with very low natural water content ($w = 3 \sim 4\%$).

The 80% and 95% joint confidence regions for the strength parameters $c' \cos \varphi'$ and $\sin \varphi'$, obtained by means of the regression analysis of the triaxial strength data are shown in Fig. 9. It can be observed that:

—there is a negative cross-correlation between the estimated values of the variables;

—the confidence interval is always very tight for the friction angle: i.e. $\varphi' = 15°$ can be virtually considered as a characteristic value for all the samples;

—the confidence interval seems to indicate a lower characteristic value of c', definitely equal to zero for shallow samples and in the order of 200 kPa for deep samples. But owing to the small number of deep samples and moreover to the discontinuous shape of the apparent strength envelope (Fig. 8), a variation of the cohesion in the range of 0–200 kPa could be considered more as a result of the natural heterogeneity of the formation than as a property strictly dependent on depth.

A set of 28 UU triaxial tests aimed at evaluating undrained strength were also carried out, but it is very likely that the results are strongly affected by the low saturation degree of the specimen. The maximum total deviator stress $(\sigma_1 - \sigma_3)_{max}$ in fact continuously increases with the

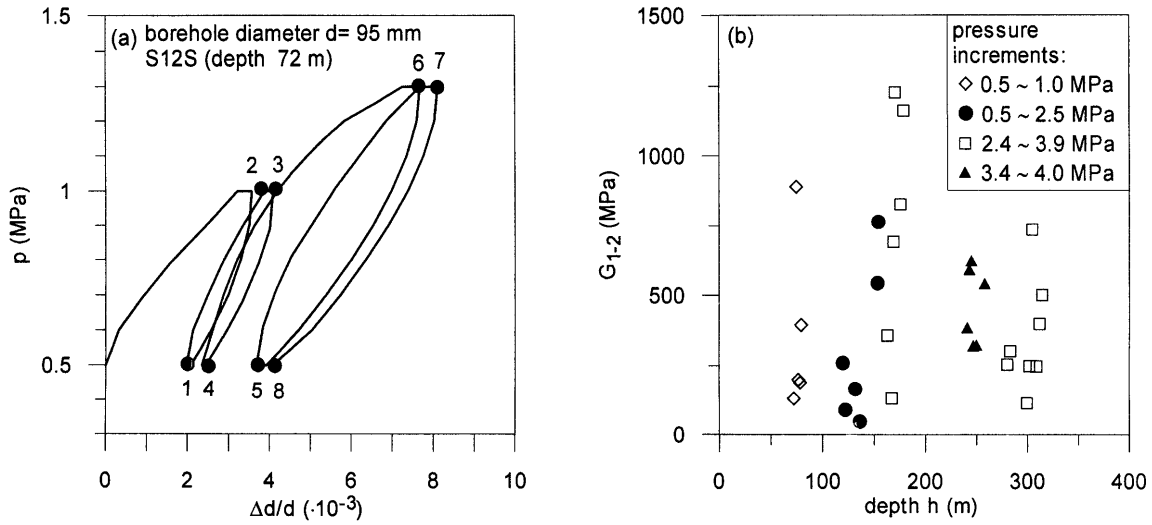

Fig. 7. Results of pressuremeter tests: typical pressure-deformation curve (a) and secant shear modulus for the first loading step G_{1-2} as a function of depth and applied pressure increment (b)

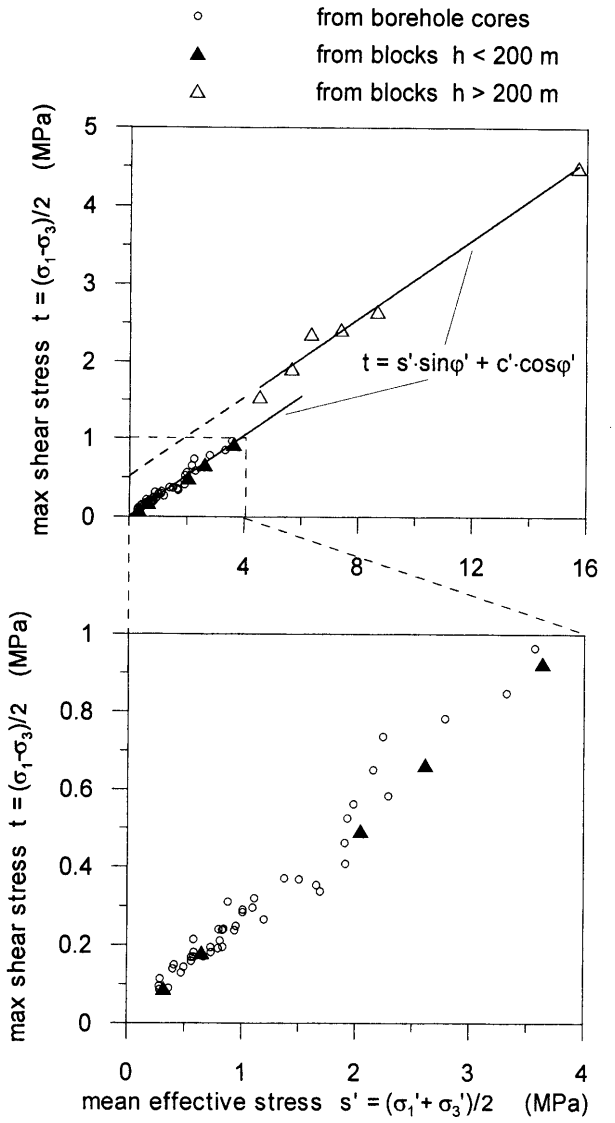

Fig. 8. Synopsis of peak shear strength data from triaxial tests and linear regression curves

applied confining stress σ_3, from an average value of 1.8 MPa for $\sigma_3 = 1$ MPa up to 4.6 MPa for $\sigma_3 = 10$ MPa.

DESIGN AND CONSTRUCTION

The design of the tunnel was based on the ADECO-RS approach (Lunardi, 2000), whose distinctive feature is to highlight the key role of tunnel face stability for the overall static conditions of the tunnel; it also introduces the principles of the observational method into tunnel design.

Full face excavation was preferred for the operational advantages it secures, such as enabling a high level of industrialized construction and safe working conditions; it also provides static benefits, mainly the possibility of closing the support ring with an invert arch immediately behind the face, and of extensively applying face reinforcement by high-power mechanized equipment.

Figure 10(a) shows a typical cross-section of the tunnel (area ~130 m^2), with the primary lining consisting of a shotcrete layer (thickness 25~30 cm) and steel sets (2 coupled 220 mm I-beams/m), including an arched strut in the invert. The final lining is in reinforced concrete (invert and sidewalls) and plain concrete (vault), with a standard

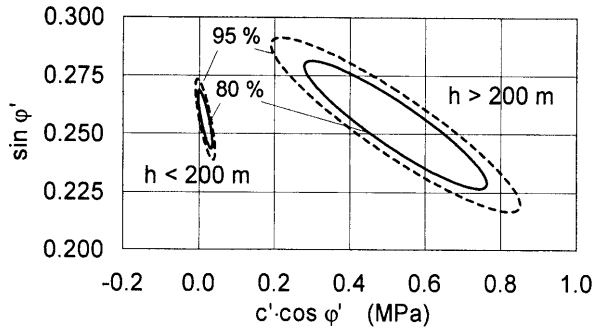

Fig. 9. 80% and 95% joint confidence regions for peak shear strength data

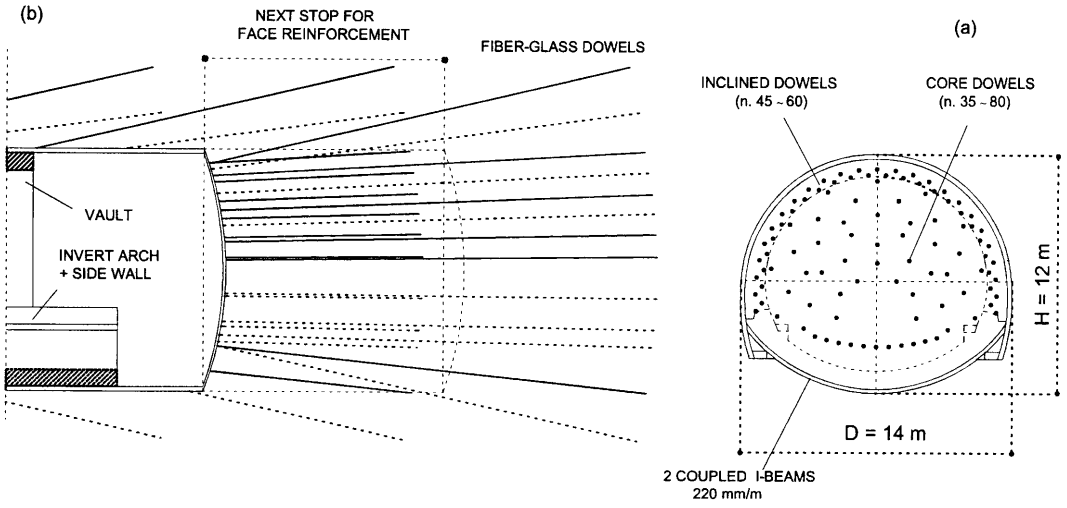

Fig. 10. Transverse (a) and longitudinal cross-section (b) of the tunnel

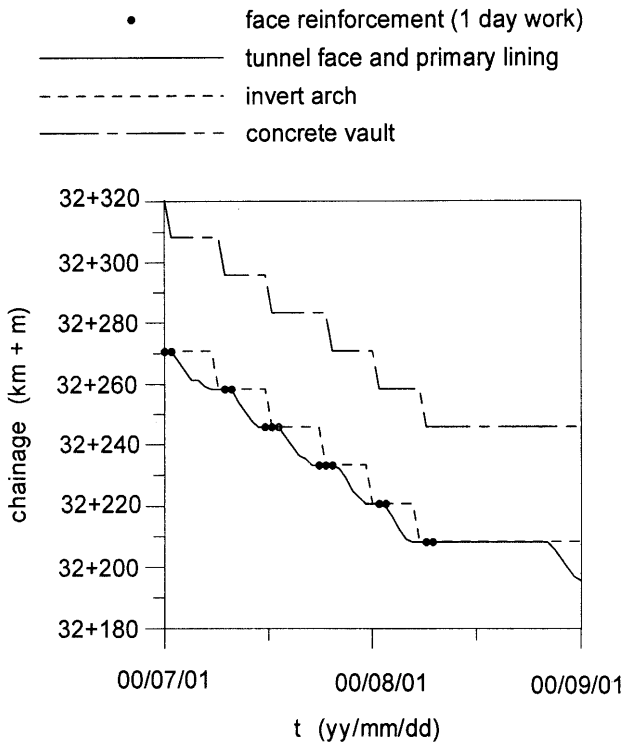

Fig. 11. Recording of the construction advance of the Raticosa tunnel during July and August 2000

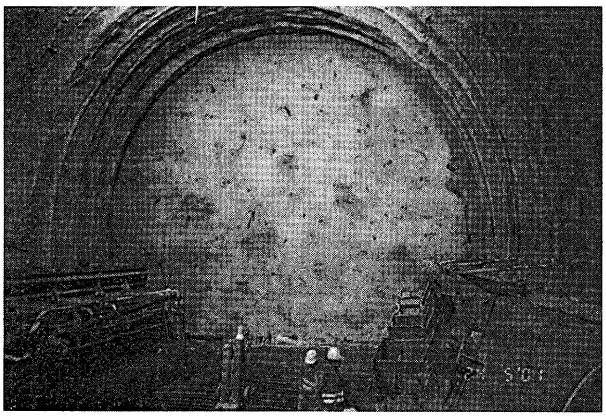

Photo 1. View of the tunnel face supported by temporary shotcrete before installation of the fiber-glass dowels

thickness of 0.9 m, increased to 1.2 m for the sections under higher overburden ($h > 350$ m).

Construction stages are better represented by the longitudinal section of the tunnel in the vicinity of the face (Fig. 10(b)) and by a typical recording of construction advance (Fig. 11).

A thin layer of shotcrete is applied to the face (Photo 1) when the excavation is stopped to allow the installation of fiber-glass dowels for safety conditions. The face is reinforced by a set of 35 ~ 80 fiber-glass dowels (diameter 32 mm, length 20 ~ 24 m) grouted by a rapid-set cement mortar; then the next round of face advance (10 ~ 12 m) is executed (Photo 2), applying a new stretch of primary lining every 1 m of excavation advance.

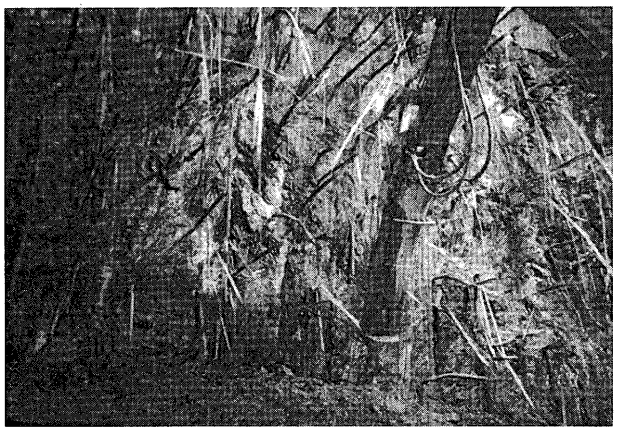

Photo 2. Detail of the tunnel face: fiber-glass dowels are easily destroyed by the hydraulic hammer

The concrete invert is cast within a one-tunnel diameter from the face, with the length of each cast segment being generally 11 m; finally the concrete lining is closed by the vault at about 30 m behind the face.

If geotechnical conditions are worse than predicted, the total number of core dowels can be increased; moreover reinforcement can be applied also beyond the excavation profile, by installing additional outer dowels with a small outward inclination.

The highest rate of reinforcement (45 inclined dowels + 50 core dowels) was actually required only for the initial stretch of the tunnel that crosses the softened and remolded shale of the paleo-landslide area at low depth. After the large ground deformation experienced while crossing the deeper section of the paleo-landslide area (*see* Section Extrusion Measurement), heavier steel sets closed by a steel strut at the invert (one 300 mm H-beam/m instead of two coupled 220 mm I-beams/m) were proposed and then applied for the whole length of the tunnel inside the Chaotic Complex. The face reinforcement applied inside the Chaotic Complex was slightly adapted to the variable geotechnical conditions encountered along the tunnel route as well: a set of 45 ~ 50 longitudinal dowels, without inclined dowels at the outer boundary, was initially applied and was found to be adequate also under the higher overburden.

Face Stability and Reinforcement Design

The design of excavation in clayey soils is usually based on the hypothesis that the material displays undrained behavior in the short term (i.e. during construction). If an isotropic in situ stress ($K_0 = 1$) is assumed, as suggested by the high overburden and low strength of the Raticosa shale, such ideal undrained conditions should be characterized by a wide plastic zone around the tunnel, where pore pressure drops significantly ($\Delta u < 0$) as a consequence of the decrease in average stress, and attains negative values as predicted by available analytical solutions based on classical elasto-plastic models (Graziani and Ribacchi, 2001).

The aforementioned model hardly applies to the case

of pervasively fissured shales, which exhibit a macroscopic opening of fissures upon stress release, with loss of saturation which removes any significant effect of inter-scale negative pore pressure (*see* also Section Geotechnical Characterization).

The mechanical behavior of the Raticosa shale within the plastic zone (i.e. zone of fissure opening and sliding) can also be represented by an equivalent continuous model of dry material. This conceptual model has inspired the stability analysis of the tunnel face and the design methods of the reinforcement system.

At the design stage, conventional stress-strain analyses of the tunnel were carried out as well, in which a "one-phase" approach (i.e., a dry material model) is used to represent clay-shale behavior, as suggested by some researchers (Comité Français de Mécanique des Roches, 2000) for stiff clay from deep deposits characterized by very low water content (say $w<10\%$, $E>2000$ MPa).

A two or three-phase model could also be applied to represent the effect of saturation-loss on the change in stiffness of the material which undergoes plastic deformations. However, this more advanced approach would be rather impractical in the context of an observational design method. On the other hand, a simpler dry material approach seems sufficiently accurate where only the stability of the tunnel is evaluated in the framework of limit analysis design; in fact it is the strength of the loosened material inside the plastic zone which mainly affects the collapse mechanism.

The minimum support pressure q_t required for face stability has been therefore evaluated by applying available limit analysis solutions (Leca and Dormieux, 1990), calculated on the basis of drained shear strength parameters c', φ'.

For a purely frictional material, upper and lower bound solutions for face stability can be represented by the expressions

$$q_t^+ \leqslant N_\gamma^+ \gamma a \tag{1a}$$

$$q_t^- \geqslant N_\gamma^- \gamma a \tag{1b}$$

where q_t is the support pressure applied to the face, γ is the unit weight of the ground and a is the radius of the tunnel. The two equations provide a bracketed estimate of the required support pressure: the smaller value being obtained by the upper bound solution (+), the greater value by the lower bound solution (−).

The cohesion of the ground can be taken into account simply by adding the term $c\cdot\cot\varphi$ onto the left side of Eq. (1), on the basis of Caquot's equivalence theorem. The domain of stable face conditions (Fig. 12) is therefore bounded by a straight line in the plane of non-dimensional variables, $c/\gamma a$ and $q_t/\gamma a$, and its equation is:

$$\frac{q_t}{\gamma a}+\frac{c\cot\varphi}{\gamma a}=N_\gamma \tag{2}$$

The non-dimensional term N_γ is a function of the friction angle φ and of the scaled depth of the tunnel h/a.

Realistic lower bound estimates, N_γ^-, for deep tunnels

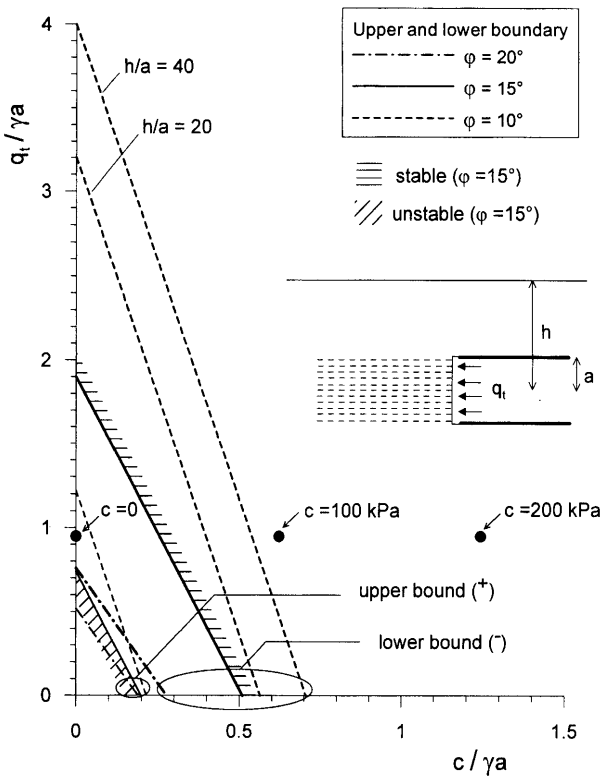

Fig. 12. Upper and lower bound estimate of the critical support pressure q_t as a function of cohesion c, for different values of the friction angle φ

are provided by the static analysis of a spherical cavity (Mandel and Halphen, 1974) by means of the characteristic lines method. N_γ^- exhibits a rapid increase with depth, and an asymptotic value is generally reached at small depths unless the friction angle is very low ($\varphi<12°$).

Upper bound kinematic 3D solutions were provided by Leca and Dormieux (1990) and were recently improved and extended by Subrin and Wong (2002). The kinematic solutions for N_γ^+ are independent of h/a (for deep tunnels).

The upper and lower boundaries have been calculated for the design value, $\varphi=15°$, of the friction angle; moreover the effect of $a\pm5°$ variability has been analyzed. The difference between the upper and the lower bound limits is very large; nevertheless, the "unsafe" upper bound estimate is probably the one closest to the real solution, as shown by centrifuge experiments (Chambon and Corté, 1990).

The maximum value of the support pressure q_t^B equivalent to the fiber-glass dowel effect is given by (Cosciotti et al., 2001)

$$q_t^B = n_b A_b f_b \tag{3}$$

where n_b represents the reinforcement ratio (i.e. number of dowels per unit area), while A_b and f_b represent the cross section area and the design axial stress of a dowel.

An equivalent support pressure on the face of 0.14 MPa is obtained for the typical pattern of 45 core dowels by assuming a design stress f_b equal to 2/3 of the

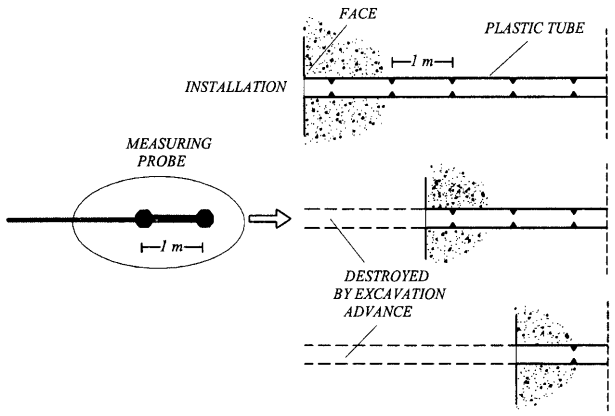

Fig. 13. Sketch of the measuring device for longitudinal displacement

dowel yield stress ($f_y = 900$ MPa), which accounts for brittle dowel behavior and poor bonding strength at the grout-shale interface.

The range of possible loading conditions is indicated in Fig. 12 by the solid circles corresponding to a support pressure $q_t = q_t^B$ and a cohesion respectively equal to 0 and 200 kPa (*see* Section Geotechnical Characterization).

Even in the absence of cohesion, the reinforcement system is capable of assuring stability; while for a cohesion higher than around 100 kPa, the face would be self-supporting.

ANALYSIS OF MONITORING DATA

The whole construction process has been performed under the constant control of a monitoring system which is based mainly on the geodetic survey of tunnel wall displacements (a measuring section almost every 30 m with 5 optical targets installed close to the face) and on axial deformation measurements. The latter are carried out by a sliding micrometer along special tubes installed from the face in the direction of the tunnel axis (Fig. 13). The initial length of the measuring tube is around 34 m but it shortens progressively because the plastic tube is being cut as the excavation advances. The remaining part of the tube in the ground, except for a short length (~1 m) closest to the face which is often excessively damaged, is nevertheless still suitable for measurements by means of the sliding micrometer.

The total number of installed tubes is enough to provide a representative picture of displacements throughout the tunnel length.

Extrusion Measurements

Figure 14 shows two typical extrusion measurements recorded at two different chainages in the Raticosa tunnel.

The longitudinal displacement profile ("extrusion" profile) is obtained by adding up the relative displacements of the reference rings along the tube, initially placed at 1 m intervals. This integration procedure starts from the far end of the tube, where the absolute displacement is assumed equal to zero, following the practice which is common with inclinometer readings.

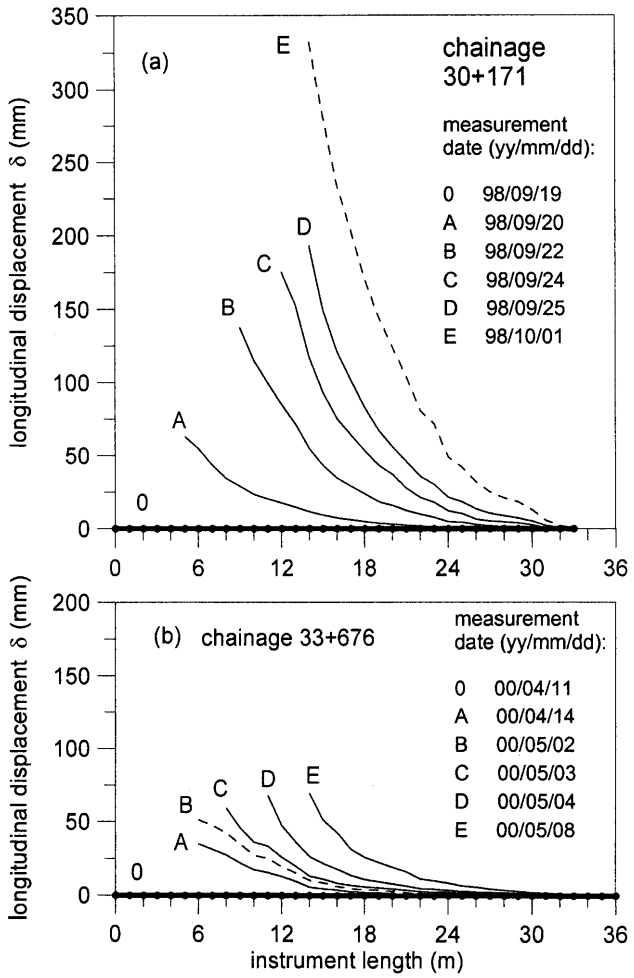

Fig. 14. Extrusions measured during face advance at two different tunnel chainages

Figure 14(a) refers to the paleo-landslide zone (overburden 30 m). The length of the tube decreased from the initial 33 m (zero reading) to the final 20 m, corresponding to the last D and E readings, taken after 13 m of face advance. Every measurement exhibits an "extrusion" which reaches a maximum at the tunnel face; extrusion values are progressively higher as the face advances, thus indicating that excavation-induced deformations affect the ground core for a distance significantly greater than 13 m.

A different trend is shown by the "extrusion" measured in the Chaotic Complex underneath a high overburden (Fig. 14(b)). The maximum extrusion is reached after a face advance of about 10 m (reading D) with no further increases in the next steps (reading E). This behaviour suggests that inside the stronger clay shale formation the influence zone of the face is limited to about 10 m.

From Fig. 14, also the effect of time-dependent deformation can be appreciated: at chainage 30+171, no excavation occurred between readings D and E, meanwhile an approx. 21-mm/day-face-extrusion increase was measured; a much smaller deformation of only 1.2 mm/

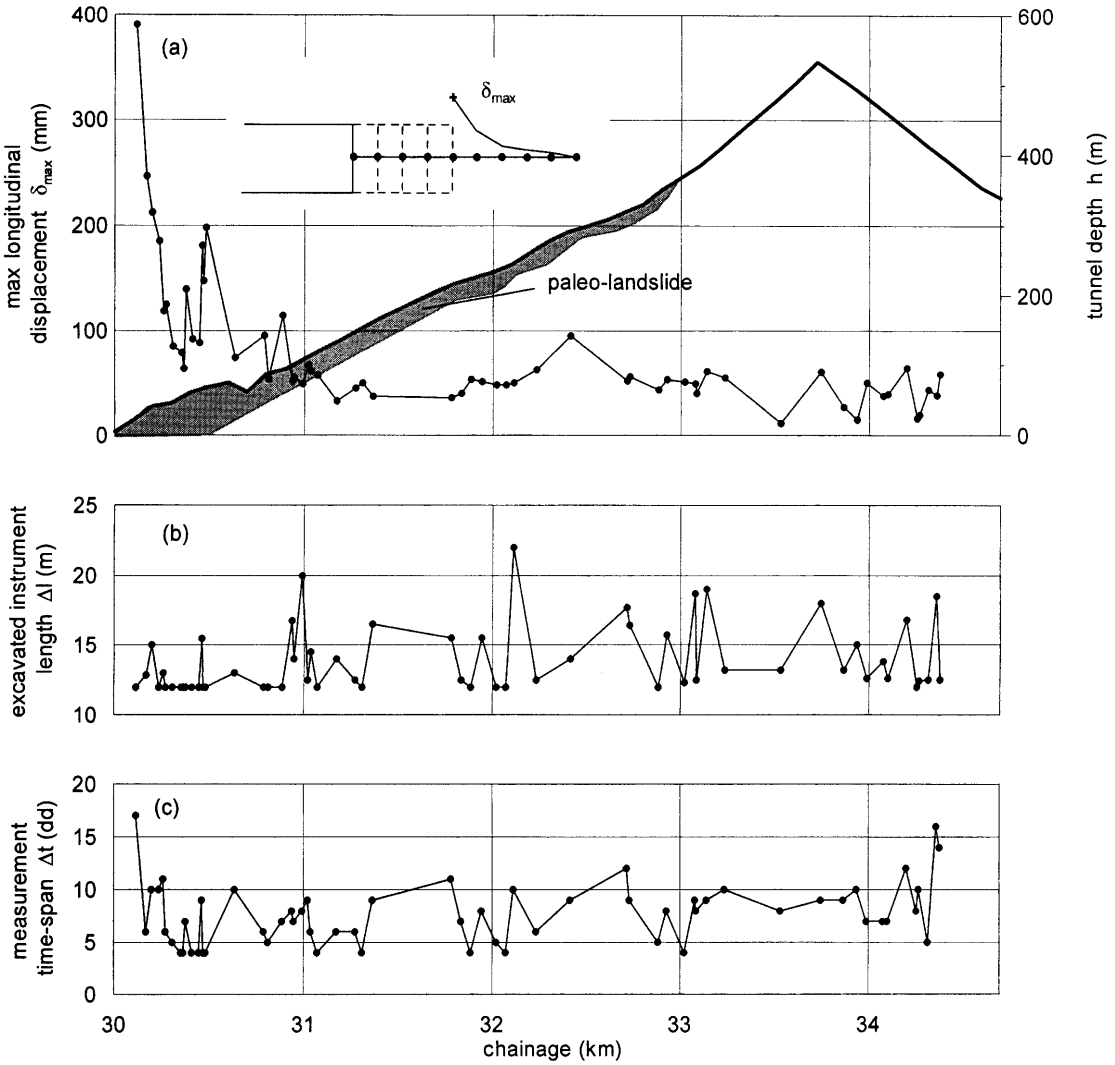

Fig. 15. Maximum longitudinal displacement (face "extrusion") measured along the tunnel route (a), corresponding excavated length Δl of the extensometer tube (b) and time elapsed, Δt, after the zero reading (c)

day was measured at chainage 33+676, during a face stop between readings A and B.

A picture of maximum extrusions δ_{max}, recorded by the various instruments installed along the tunnel route, is represented in Fig. 15. In order to obtain more homogeneous and comparable data, only extrusion measurements relative to the excavated length of the instrument $\Delta l > 12$ m have been considered in Fig. 15. In fact, the face could have experienced an even larger extrusion than that recorded by the measurement system. The effective Δl values and the time Δt that elapsed between the zero reading and the final reading of each instrument are therefore represented as well.

At low tunnel depths, i.e. in the paleo-landslide area, maximum measured extrusions attain values even larger than 200 mm, which can be interpreted as a sign of actually unstable face conditions, as confirmed by the high deformation rate during face stops. On the contrary, inside the Chaotic Complex the maximum extrusion values are always of the order of 50 mm, almost independent of tunnel depth, thus denoting substantially stable face conditions.

Convergence Measurements

Figure 16 summarizes maximum convergence, crown settlements and longitudinal displacements measured by each monitoring section along the tunnel route. Apart from maximum values exceeding 120 mm in the paleo-landslide area, the average convergence is around 40 mm in the tectonized shale.

Data scatter is higher for convergence than for extrusion: this cannot be explained only by different levels of accuracy between the geodetic survey and the sliding micrometer measurements. A major role must be attributed to interaction with the primary lining, which is quite sensitive to installation unevenness.

Despite the data scatter, the monitoring data (Fig. 16) show a small but significant influence of the overburden on convergence; a linear regression of the data indicates an increase of about 5 mm for every 100 m of depth. A similar trend is shown by the longitudinal displacements.

By observing that the average horizontal displacement of points 1 and 5 on the sidewalls is almost equal to the vertical displacement of point 3 (crown), it is argued that the bending distortion of the lining is limited; therefore

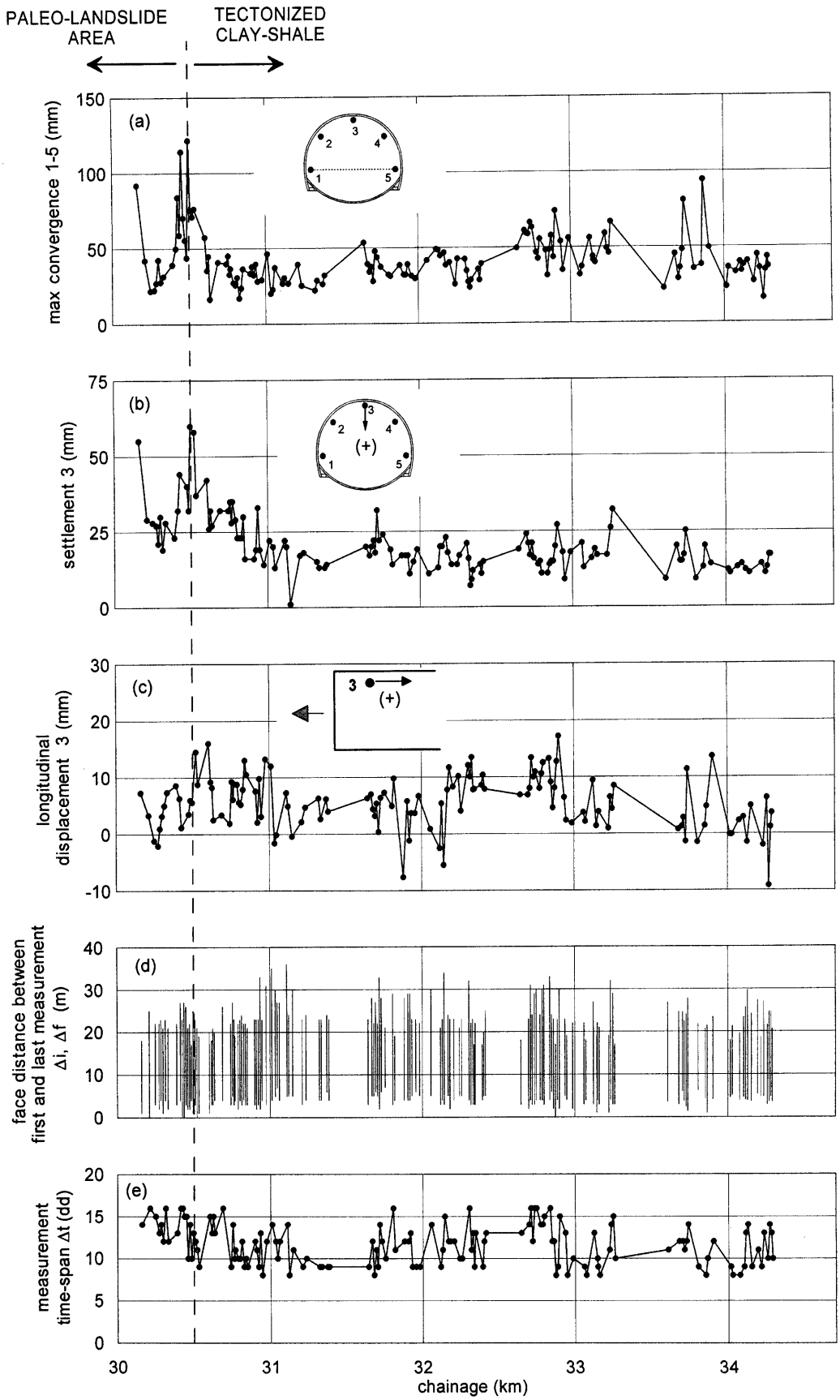

Fig. 16. Maximum horizontal convergence (a), crown settlement (b) and longitudinal displacement (c); distances, Δi, Δf, between the face and the monitoring section at the time of initial and final readings; (d), time elapsed, Δt, between initial and final measurements (e)

there is an almost uniform hoop stress distribution between the inner and outer sides of the lining.

Longitudinal displacements of the different points within the cross-section of the tunnel are almost equal. The whole sections tend to move in the same direction of the face, but the displacement magnitude is much smaller.

A rough interpretation of the convergence data has been based on the curve-fitting technique proposed by Sulem et al. (1987).

Tunnel closure is represented by an empirical law $C(x, t)$, which takes into account the effect of both face distance x and the time-dependent behavior of the ground:

$$C(x,t)=C_{\infty,x}\left\{1-\left[1+\frac{x}{X}\right]^{-2}\right\} \times\left\{1+m\left[1-\left(1+\frac{t}{T}\right)^{-n}\right]\right\} \qquad (4)$$

where t is the time elapsed since the face passed through the monitoring section.

Relationship (4) depends on five parameters: $C_{\infty,x}$ ("instantaneous closure") and X (a distance related to tunnel radius R) which control the face effect, and m, T and n for the time-dependent contribution.

The free parameters can be determined by a non-linear regression of experimental data for each monitoring section where a set of at least $k=15\sim20$ readings are available, starting from a "zero" reading made close to the tunnel face (distance x_0) at time t_0. The set of k equations to be solved, according to the minimum squares method, therefore assumes the form:

$$\Delta C_{i,\text{measured}}=C(x_i, t_i)-C(x_0, t_0) \quad i=1, k. \qquad (5)$$

To reduce problems of ill-conditioning of the system of Eq. (5), exponent n was fixed at a value of 0.3, as suggested by Sulem et al. (1987).

Figure 17 shows two examples of convergence curve fitting by means of Eq. (4), respectively for a monitoring section located in the completely softened shale (chainage 30+343, overburden 50 m), and another one deep inside the Chaotic Complex (chainage 32+998, overburden 365 m). In the lower part of the graphs, the distance between excavation face and the monitoring section as a function of time is also represented to make the interpretation of the observed behavior easier.

The estimated values of the regression parameters, also reported in Fig. 17, indicate a remarkable amount of time-dependent convergence, whose asymptotic values, controlled by the parameter m, is equal to $1.8\div2.4$ times the convergence due to the face advance.

Time-dependent deformations can be clearly evidenced during a period of excavation pause, like the 20-day stop reported in Fig. 17(b). In this case, when the face stopped at a distance of about 26 m from the monitoring section, the corresponding increase in convergence was about 15 mm; this measured value is well reproduced by the fitting procedure. This kind of behavior, observed also in other monitoring sections, highlights how important it is

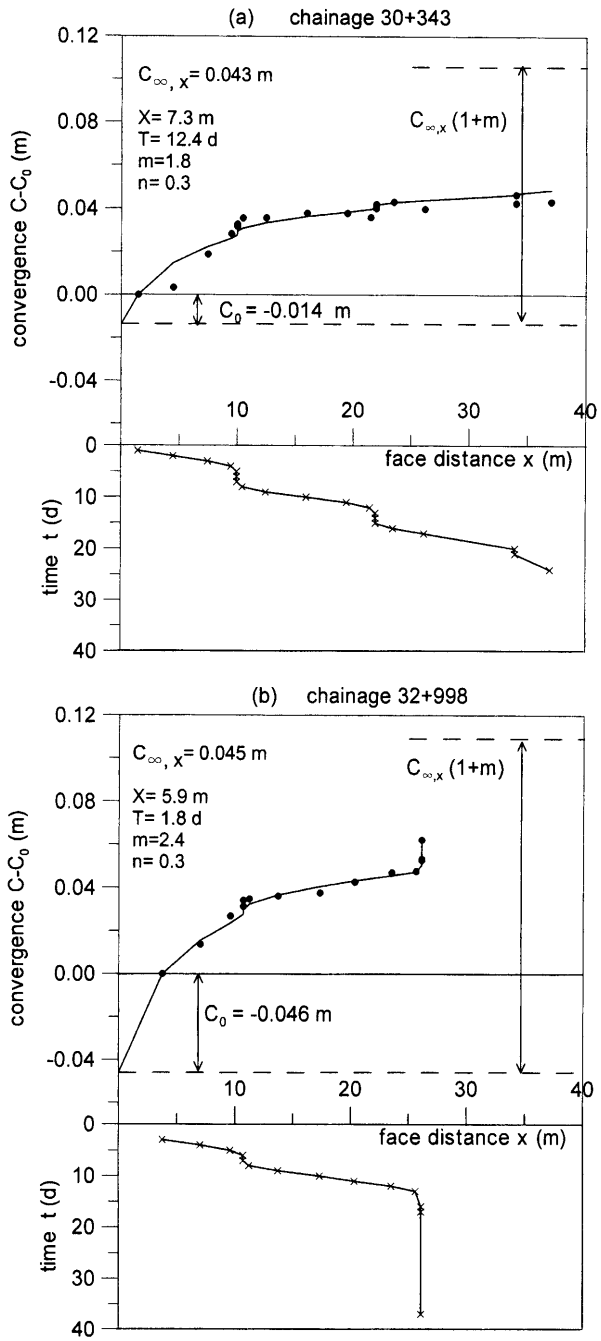

Fig. 17. Curve fitting of convergence measurements at two monitoring sections

to closely respect the construction-time schedule in order to prevent overloading of the primary lining before the final setting of the concrete lining.

CONCLUSIONS

The analysis of the excavation performance of the Raticosa railway tunnel under the Apennine range contributes to a better understanding of the behavior of a typical tectonized clay-shale formation (widespread throughout peninsular Italy) under high overburden and in a paleo-landslide area. Furthermore, the validity of the adopted excavation method, based on full face excava-

tion associated with face reinforcement by means of fiber-glass dowels and with a primary lining made of shotcrete and steel sets, has been confirmed by the monitoring results.

Geotechnical characterization of the tectonized clay-shale required several laboratory and in situ tests carried out at the exploration and design stages and needed continuous updating during tunnel excavation. Many difficulties were caused by sensitivity of the fissured clay material to sampling and specimen preparation. The strength data indicate a typical value for the friction angle of 15° while the estimated cohesion values show a wider range of variation with a characteristic lower limit equal to zero.

Stress-strain analysis of the tunnel construction was not addressed in this paper, only some topics related to face stability and reinforcement design were examined. A limit analysis, aimed at assessing the minimum support pressure required for face stability, indicated that the adopted face reinforcement is adequate even for the case of negligible ground cohesion.

The ground behavior during tunnel construction was monitored by means of longitudinal displacement measurements ahead of the tunnel face (extrusion measurements) and by geodetic surveys of tunnel wall displacements (convergence measurements). The paleo-landslide area was characterized by very high values of extrusion and convergence as well as by high deformation rates during the excavation stops, thus indicating that face conditions were close to instability. Ground deformation caused by tunnel excavation was lower at higher depths inside the Chaotic Complex, and face extrusion settled to an almost constant value irrespective of tunnel depth. Tunnel convergence measurements, albeit characterized by larger scatter, indicated a small but significant influence of the tunnel depth. The time-dependent convergence was estimated to be about 2 times the convergence due to face advance. Such a remarkable amount of delayed ground deformations clearly demonstrates the importance of complying with the time-schedule for installing the final lining in order to avoid overloading of the primary lining.

ACKNOWLEDGEMENTS

The authors would like to acknowledge Dott. Castellani, Ing. Meistro and Dott. Carrara of CAVET and Dott. Balestrieri and Dott. Negri of 3S for having provided the monitoring data of the Raticosa tunnel and Ing. Gambelli and Ing. Cascino of ITALFERR for their cooperation during the activities at the tunnel site.

REFERENCES

1) AGI (Italian Geotechnical Association) (1985): Some Italian experiences on the mechanical characterization of structurally complex formations. *4th ISRM Congr., Montreux*, **1**, 827–846.
2) Chambon, P. and Corté, J. F. (1990): Stabilité du front de taille d'un tunnel dans un milieu frottant—approche cinématique en calcul à la rupture, *Rev. Franç. Géotech.*, **51**, 51–59.
3) Comité Français de Mécanique des Roches (2000): *Manuel de Mécanique des Roches, Tome 1: Fondements*. Paris, Ecole des Mines, 265.
4) Cosciotti L., Lembo Fazio, A., Boldini, D. and Graziani, A. (2001): Simplified behavior models of tunnel faces supported by shotcrete and bolts. *Int. Symp. Modern Tunneling Science and Technology* (eds. by Adachi et al.), **1**, 407–412.
5) Gambelli, C. (1999): Bologna-Florence high speed railway project—cooperation between client and contractor. *Felsbau*, **17**, 367–373.
6) Graziani, A. and Ribacchi, R. (2001): Short and long-term load conditions for tunnels in low permeability ground in the framework of the convergence-confinement method. *Int. Symp. Modern Tunneling Science and Technology* (eds. Adachi et al.), **1**, 83–88.
7) Leca, E. and Dormieux, L. (1990): Upper and lower bound solutions for the face stability of shallow circular tunnels in frictional material, *Géotechnique*, **40** (4), 581–606.
8) Lunardi, P. (2000): The design and construction of tunnels using the approach based on the analysis of controlled deformation in rocks and soils, *Tunnels and Tunneling Int.*, **5**, 3–29.
9) Lunardi, P. and Focaracci, A. (1999): The Bologna to Florence high speed railway line: progress for underground. *Challenges for the 21st Century* (eds. by Alten et al.), 585–593.
10) Mandel, J. and Halphen, B. (1974): Stabilité d'une cavité sphérique souterraine. *3rd ISRM Congr.*, Denver: (2B), 1028–1032.
11) Picarelli, L., Olivares, L., Di Maio, C., Silvestri, F., Di Nocera, S. and Urciuoli, G. (2002): Structure, properties and mechanical behaviour of the highly plastic intensely fissured Bisaccia Clay Shale in Italy. *Characterisation and Engineering Properties of Natural Soil* (eds. by Tan et al.), **2**, 947–982.
12) Subrin, D. and Wong, H. (2002): Stabilité du front d'un tunnel en milieu frottant: un nouveau mécanisme de rupture 3D. *C. R., Mécanique*, **330**, 513–519.
13) Sulem, J., Panet, M. and Guenot, A. (1987): Closure analysis in deep tunnels. *Int. J. Rock Mech. Min. Sci. and Geomech. Abstr.*, **24** (3), 145–154.
14) Wittke, W. (2000): Stability analysis for tunnels. *Verlag Gluckauf GmbH*, Essen, 415.